# SU(2) symmetry in a realistic spin-fermion model for cuprate superconductors

T. Kloss, X. Montiel, and C. Pépin

Phys. Rev. B **91**, 205124 — Published 22 May 2015

DOI: 10.1103/PhysRevB.91.205124

# SU(2)-symmetry in a realistic spin-fermion model for cuprate superconductors

T. Kloss[1,2], X. Montiel[1,2], C. Pépin[1]
[1]*IPhT, L'Orme des Merisiers, CEA-Saclay, 91191 Gif-sur-Yvette, France and*
[2]*IIP, Universidade Federal do Rio Grande do Norte, Av. Odilon Gomes de Lima 1722, 59078-400 Natal, Brazil*
(Dated: May 01, 2015)

We consider the Pseudo-Gap (PG) state of high-$T_c$ superconductors in form of a composite order parameter fluctuating between $2\mathbf{p}_F$-charge ordering and superconducting (SC) pairing. In the limit of linear dispersion and at the hotspots, both order parameters are related by a SU(2) symmetry and the eight-hotspot model of Efetov *et al*. [Nat. Phys. **9**, 442 (2013)] is recovered. In the general case however, curvature terms of the dispersion will break this symmetry and the degeneracy between both states is lifted. Taking the full momentum dependence of the order parameter into account, we measure the strength of this SU(2) symmetry breaking over the full Brillouin zone. For realistic dispersion relations including curvature we find generically that the SU(2) symmetry breaking is small and robust to the fermiology and that the symmetric situation is restored in the large paramagnon mass and coupling limit. Comparing the level splitting for different materials we propose a scenario that could account for the competition between the PG and the SC states in the phase diagram of high-$T_c$ superconductors.

PACS numbers: 74.40.Kb 74.20.-z 74.25.Dw 74.72.Kf

## I. INTRODUCTION

Reflecting our rather poor understanding of the physics of cuprate superconductors, two kinds of theories are still debating whether the final solution for this problem will be a "bottom-up" approach based on a strong coupling theory[1–3] or rather a "top-down" approach, where symmetries and proximity to a Quantum Critical Point (QCP) plays a dominant role[4–7]. The recently proposed Eight Hot Spots (EHS) model is a promising "top-down" approach to cuprate superconductors[8,9]. It reduces the Fermi surface to only eight points on the anti-ferromagnetic (AF) zone boundary and taking long-range AF fluctuations between them into account. When the dispersion is linearized at the hot spots, one observes surprisingly that an SU(2) symmetry relating the $d$-wave SC channel (Cooper pairing) to the $d$-wave bond order, or Quadrupolar Density Wave (QDW), (charge channel) is present. Moreover, an imposant pre-emptive instability (of order of 0.6 J, where J is the AF energy scale) in the form of a composite SU(2) order parameter emerges, that has been identified as a good candidate for the pseudo-gap (PG) state of those compounds[9–12]. Motivated by an impressive set of new experimental results[13–22], this theory points out to the emerging idea that charge order is most certainly a key player in the physics of cuprate superconductors, in addition to AF order, $d$-wave SC state and the Mott insulator phase. Angle-resolved photoemission spectroscopy (ARPES) experiments confirm as well the presence of modulations in the SC state for underdoped Bi2201[23,24] and has been interpreted either in terms of charge order or Pairing Density Wave (PDW) inside the PG phase[25–28]. Finally, we like to mention the recent interpretation of Raman resonances by a collective SU(2) mode which is the first experimental result that supports the idea of a composite PG[29].

The idea of an emerging SU(2) symmetry belongs to a wide class of theories which explain the PG phase of the cuprates through the notion of degenerate symmetry states between the $d$-wave SC order and another partner. Maybe the most famous attempt to such a unification has been the SO(5) theory which relates the $d$-wave SC state to the AF order[30]. Not less famous is the SU(2) symmetry which relates the SC $d$-wave order to the $\pi$-flux phase of orbital currents[1]. In both cases, the key question was to argue that the energy splitting between the two orders was small enough so that thermal effects would restore the symmetry above $T_c$ and below $T^*$, which are the SC and the PG critical temperatures. The same question holds here for the SU(2) symmetry relating $d$-wave and QDW order. Although the EHS model in its linearized version verifies the symmetry exactly, it is not clear if a more realistic Fermi surface, including curvature and the whole band structure, will induce small or large energy splitting. Moreover, the EHS model relies on long-range AF fluctuations which mediate the interactions, but the experimental observation points out to short-range AF correlations which potentially will gap a whole part of the Fermi surface, as depicted in Fig. 1. A theory for "hot regions" instead of "hot spots" is thus needed.

In this paper we address carefully all these issue by evaluating the SU(2) splitting on realistic Fermi surfaces, for the two distinct components of the composite order parameter: the $d$-wave $\chi$-field in the charge sector (which forms the QDW order in the EHS model) and the $d$-wave $\Delta$-field describing the SC pairing sector. We find that the splitting of the SU(2) symmetry increases with the mass of the paramagnons, but decreases with the strength of the coupling constant between AF fluctuations and conduction electrons. This opens a wide regime of parameters where the splitting is minimal – of the order of a few percents – and where the SU(2) symmetry is expected to be recovered through thermal effects in a regime of temperatures $T_c < T < T^*$. Above the PG temperature $T^*$ all traces of the short-range charge and SC field have disappeared. Of course the SU(2) symmetry holds in the whole temperature range between $T_c$ and $T^*$, hence subleading charge instabilities which occur below $T^*$ do have their SU(2) partners in the form of Pairing Density Waves (PDW)[31,32]. We also study the effects of the Fermi surface shape in breaking the SU(2) symmetry – which is only preserved in the EHS model with a

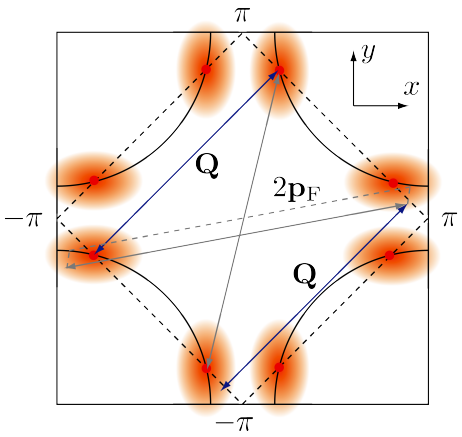


FIG. 1. (Color online) Schematic Fermi surface of hole-doped superconductors in the first Brillouin zone of a square lattice. The order parameters spatially extent over hot regions, that are centered around the hotspots positions and which are coupled by the $2\mathbf{p}_F$ and the AFM coupling $\mathbf{Q}$ to opposed regions.

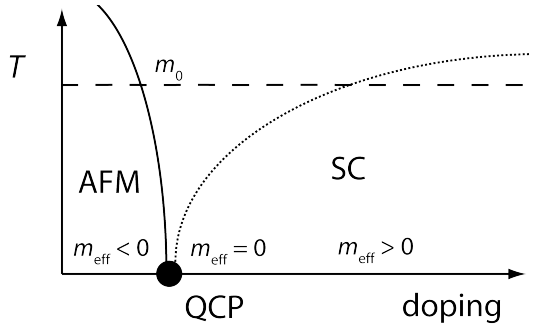


FIG. 2. Schematic phase diagram of hole-doped cuprate superconductors. The effective mass of the paramagnon propagator $m_{\rm eff}$ serves as as measure for the distance to the quantum critical point QCP. In the SC phase $m_{\rm eff}$ is positive and vanishes at the QCP to become negative in the AFM phase. The bare mass $m_{\rm bare}$ is defined far away from criticality at some higher temperature, indicated by the dashed line.

linearized dispersion. We find that the splitting is small away from the points where $\chi$ and $\Delta$ are maximal. In the physical situation of a large paramagnon mass and also strong coupling, the maximum of $\chi$ moves towards the zone edge leading to bond order parallel to the $x$-$y$ axes. All these findings point to the realization that, while being a secondary instability to AF ordering, charge order is a key player in the physics of the PG phase of the cuprates.

## II. MODEL

We start from the spin-fermion model[8,9,31] with Lagrangian $L = L_\psi + L_\phi$, where

$$L_\psi = \psi^* \left(\partial_\tau + \varepsilon_k + \lambda\phi\sigma\right)\psi\,, \tag{1a}$$

$$L_\phi = \frac{1}{2}\phi D^{-1}\phi + \frac{u}{2}\left(\phi^2\right)^2\,. \tag{1b}$$

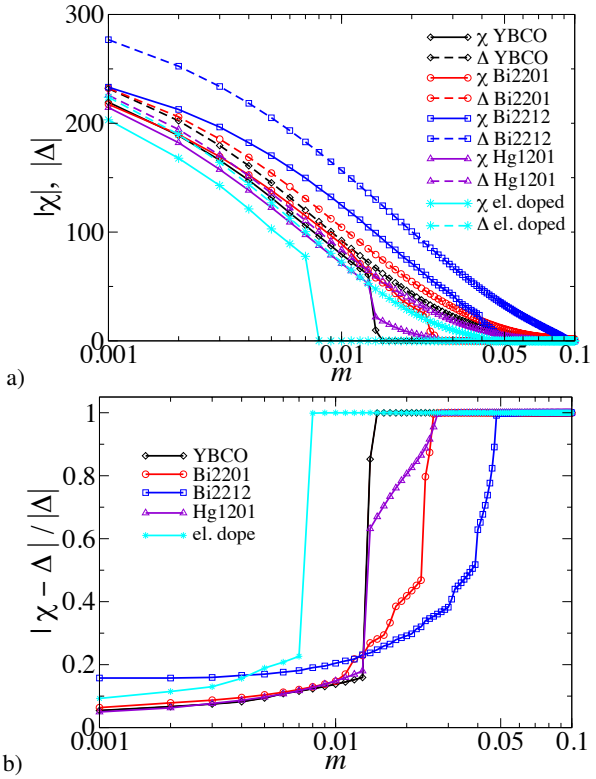


FIG. 3. (Color online) Panel a): Variation of the maximum value of the gap functions $|\chi|$ and $|\Delta|$ as a function of the mass $m$. Note that in all materials the $2\mathbf{p}_F$ pairing in terms of $|\chi|$ vanishes abruptly, whereas the SC pairing in terms of $|\Delta|$ approaches zero asymptotically when the paramagnon mass $m$ is increased. Panel b): Variation of the level splitting as a function of the mass $m$. In both panels $\lambda = 44$.

The fermionic field $\psi$ describes the electrons which are coupled via $L_\phi$ to spin waves described by the bosonic field $\phi$. The effective spin-wave propagator is $D_q^{-1} = \gamma|\omega| + |\mathbf{q}|^2 + m$ where $m$ is the paramagnon mass which vanishes at the QCP and $\gamma$ a phenomenological coupling constant, which we estimate from its form in the EHS model[9] to be of the order $10^{-5}$. For notational reasons we also write $q \equiv (i\omega, \mathbf{q})$. Neglecting the spinwave interaction ($u = 0$) one can formally integrate out the bosonic degrees of freedom. In the spin boson model, this generates an effective spin-spin interaction of the form

$$S_{\rm int} = -\sum_q \bar{J}_q \vec{S}_q \vec{S}_{-q}. \tag{2}$$

It is convenient to use a fermionic representation of the spin operator $\vec{S}$ and consider in the following only the paramagnetically ordered phase in $z$-direction, so that $\bar{J} = 3/2J$. The partition function then writes $Z = \int \mathscr{D}[\Psi]\exp(-S_0 - S_{int})$ with

$$S_0 = \sum_{k,\sigma} \Psi_k^\dagger G_{0,k}^{-1} \Psi_k, \tag{3a}$$

$$S_{int} = -\sum_{k,k',q,\sigma} J_q \psi_{k,\sigma}^\dagger \psi_{k+Q+q,\bar{\sigma}} \psi_{k',\bar{\sigma}}^\dagger \psi_{k'-q-Q,\sigma}. \tag{3b}$$

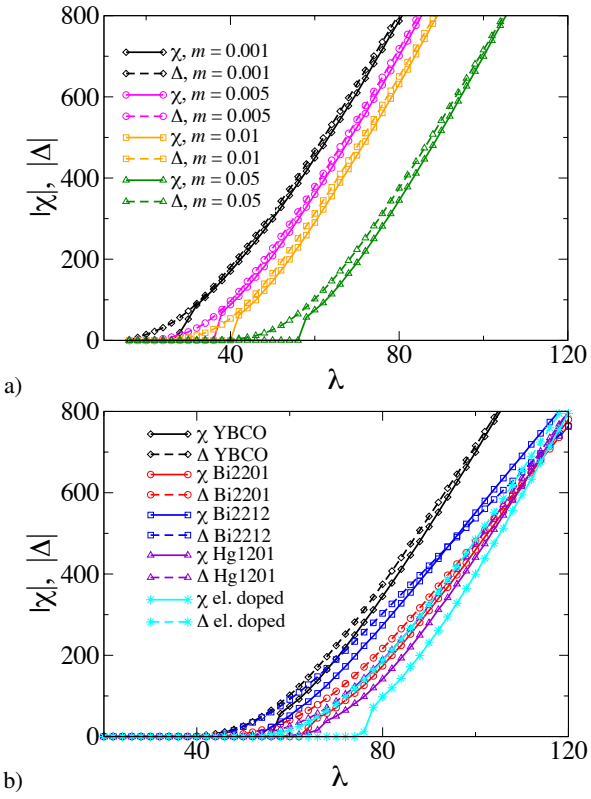


FIG. 4. (Color online) Panel a): Variation of the maximum value of the gap functions $|\chi|$ and $|\Delta|$ in YBCO as a function of the coupling $\lambda$ for different masses $m$. Panel b): Variation of the maximum value of the gap functions $|\chi|$ and $|\Delta|$ for different compounds as a function of the coupling $\lambda$ for the mass $m = 0.5$.

where the bare propagator is

$$\hat{G_0}_k^{-1} = \mathrm{diag}(i\omega - \varepsilon_{\mathbf{k}}, i\omega + \varepsilon_{-\mathbf{k}-\mathbf{p}}, i\omega - \varepsilon_{\mathbf{k}+\mathbf{p}}, i\omega + \varepsilon_{-\mathbf{k}}), \quad (4)$$

and the spinor field $\Psi_k = (\psi_{k,\sigma}, \psi^\dagger_{-k-p,\bar{\sigma}}, \psi_{k+p,\sigma}, \psi^\dagger_{-k,\bar{\sigma}})^T$. Furthermore, $J_q^{-1} = 4D_q^{-1}/3\lambda^2$, $\sigma \in \{\uparrow,\downarrow\}$ labels the spin, $\mathbf{Q} = (\pi,\pi)^T$ is the AFM ordering vector and $\mathbf{p}$ stands for the $2\mathbf{p}_\mathrm{F}$ vector, as depicted in Fig. 1. Note that the chemical potential $\mu$ is implicitly subtracted from the dispersion $\varepsilon_{\mathbf{k}}$. We select the SC and the $2\mathbf{p}_\mathrm{F}$ channel by introducing the two order parameters

$$\Delta_k = \langle \psi^\dagger_{k,\sigma} \psi^\dagger_{-k,\bar{\sigma}} \rangle, \qquad \chi_k = \langle \psi^\dagger_{k,\sigma} \psi_{k+p,\sigma} \rangle. \quad (5)$$

The interaction $S_1$ is now decoupled by means of a Hubbard-Stratonovich transformation. The partition function becomes (up to a normalization factor)

$$Z = \int \mathscr{D}[\Psi]\mathscr{D}[\Delta,\chi] \exp[-S_0 - S_{1,eff}]. \quad (6)$$

The effective interaction is

$$S_{1,eff} = \sum_{k,q,\sigma} \left[ J_q^{-1} \chi^\dagger_k \chi_{\bar{k}+q} + J_q^{-1} \Delta^\dagger_k \Delta_{\bar{k}+q} \right] - \sum_{k,\sigma} \Psi^\dagger_k \hat{M}_k \Psi_k, \quad (7)$$

with $\bar{\mathbf{k}} = \mathbf{k} + \mathbf{Q}$ and the matrix $\hat{M}$ is

$$\hat{M}_k = \begin{pmatrix} & \hat{m}_k \\ \hat{m}_k^\dagger & \end{pmatrix}, \qquad \hat{m}_k = \begin{pmatrix} -\chi_k & -\Delta_k \\ -\Delta^\dagger_{k+p} & \chi_{-k} \end{pmatrix}. \quad (8)$$

The fermions in Eq. (6) can now be integrated out so that the partition function becomes

$$Z = \int \mathscr{D}[\hat{M}] \exp\Big[ -\frac{1}{4} \sum_{k,q} \mathrm{Tr} J_q^{-1} \hat{M}_{\bar{k}+q} \hat{M}_k + \frac{1}{2} \sum_k \mathrm{Tr} \log \hat{G}_k^{-1} \Big], \quad (9)$$

with $\hat{G}^{-1} = \hat{G}_0^{-1} - \hat{M}$. After functional differentiation of the free energy $F = -T \ln Z$ with respect to $\hat{M}_k$ we obtain the MF equations in matrix form

$$\hat{M}_k = \sum_{k'} J_{\bar{k}-k'} \hat{G}_{k'}. \quad (10)$$

The matrix equation can now be projected onto the different components. We will consider here the case of two competing order parameters which can not be non-zero at the same point in $\mathbf{k}$ space. Therefore, we consider the equation for $\Delta$ with $\chi = 0$ and vice versa. The gap equations follow as

$$\Delta_k = T \sum_{\omega',\mathbf{k}'} J_{\bar{k}-k'} \frac{\Delta_{k'}}{\Delta^2_{k'} + \varepsilon^2_{\mathbf{k}'} + \omega'^2}, \quad (11a)$$

$$\chi_k = -\Re T \sum_{\omega',\mathbf{k}'} J_{\bar{k}-k'} \frac{\chi_{k'}}{(i\omega' - \varepsilon_{\mathbf{k}'})(i\omega' - \varepsilon_{\mathbf{k}'+\mathbf{p}}) - \chi^2_{k'}}. \quad (11b)$$

To solve these equations numerically, $\varepsilon_{\mathbf{k}}$ is parametrized in tight-binding approximation with the following parameters: YBCO[33] (parameter set tb2), Bi2201[34], Bi2212[35] and Hg1201[36] and for electron doped cuprates[37]. The momentum sums in Eq. (11) are then carried out by discretizing the $\mathbf{k}$-space by rectangular and equidistant grids. To keep the numerical computations tractable we neglect the frequency dependence of $\chi$ and $\Delta$[38]. The Matsubara sums are then carried out exactly in the limit $T \to 0$ and the momentum sums are performed over $200 \times 200$ points and over one Brillouin Zone (BZ). Moreover, note that the $2\mathbf{p}_\mathrm{F}$ vector which connects two opposed FS points at $\pm\mathbf{p}_\mathrm{F}/2$ depends on the external momentum $\mathbf{k}$ in Eq. (11) and is only properly defined on the FS. Since we expect that the main contribution to the momentum sum in Eq. (11) comes however from the hot-spot region, we make the approximation to take the $2\mathbf{p}_\mathrm{F}$ vector constant and take the $2\mathbf{p}_\mathrm{F}$ from the hotspot for arbitrary points in the first BZ, as depicted in Fig. 1. Throughout this article, we use 10% hole filling (respectively 10% electron filling in the electron doped case) and the bandgap is $10^4$ K. To evaluate the strength of the SU(2) symmetry, we study the level splitting $|\chi - \Delta|/\Delta$. This parameter afford the study of the relative amplitude between the QDW and SC order parameter, $\chi$ and $\Delta$. It vanishes for a perfect SU(2) symmetry and becomes closer to one for a complete SU(2) symmetry breaking. From the Lagragian we find that $\phi\lambda$ has dimension of an energy and $\phi \sim m^{-1/2}$. To estimate the coupling strength, we evaluate an effective energy via $E_\mathrm{eff} = \phi\lambda \sim m^{-1/2}\lambda$ and away from criticality $E_0 \sim m_0^{-1/2}\lambda$ where we take $m_0 = 1$ as bare mass, compare Fig. 2.

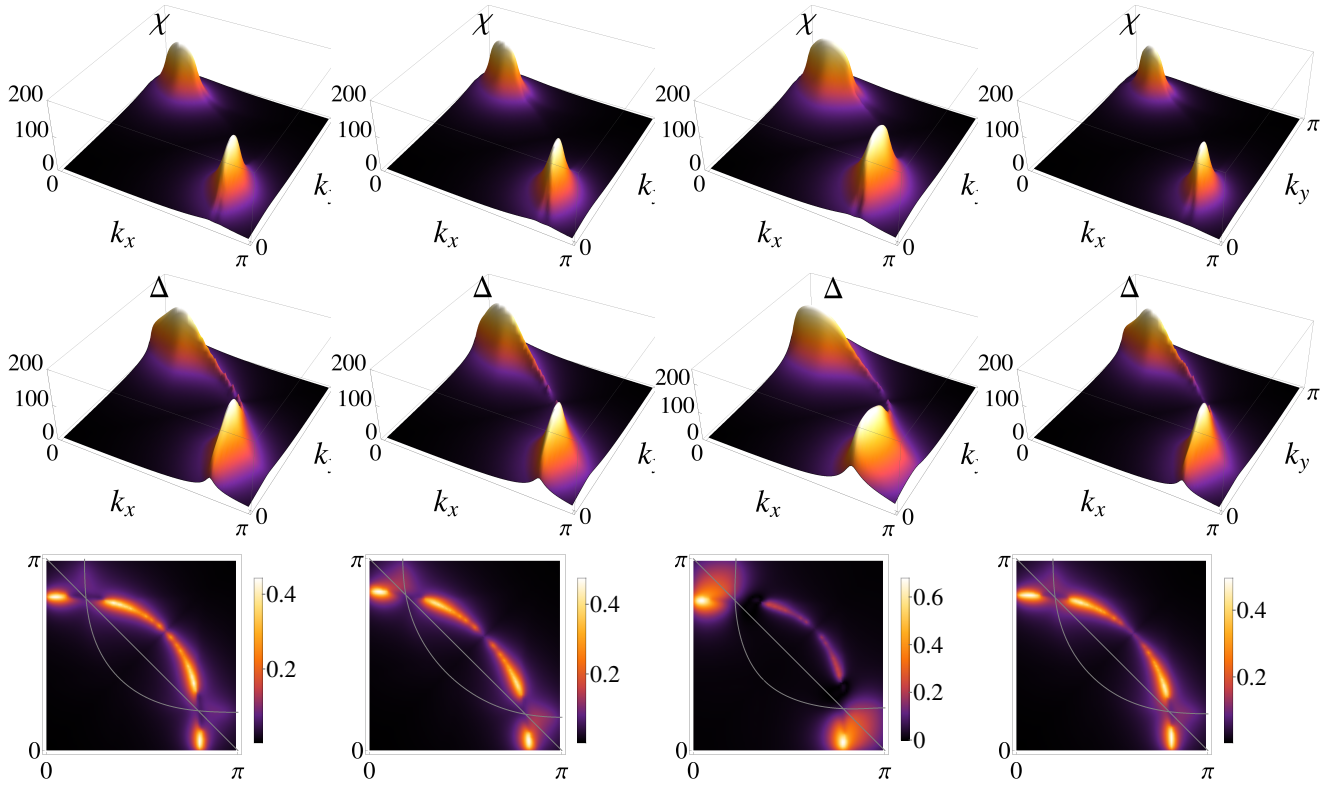


FIG. 5. (Color online) Gap functions $|\chi|$, $|\Delta|$ and $|\chi-\Delta|/|\Delta_{\max}|$ (from up to down) for different materials in the first BZ. The compounds are (from left to right): YBCO, Bi2201, Bi2212 and Hg1201. The figures correspond to the small mass and small coupling limit ($\lambda = 40$ and mass $m = 10^{-3}$; note that the bare coupling is small w.r.t. the renormalized one $E_0 \simeq 40\,\mathrm{K}$ and $E_{\mathrm{eff}} = 1265\,\mathrm{K}$) that is most unfavorable for the SU(2) symmetry.

## III. RESULTS AND DISCUSSION

### A. Mass and coupling dependence on level splitting

In order to test the effect of the curvature on the level degeneracy, we have plotted in Fig. 3a) the variation of the maxima of $\chi$ and $\Delta$ with the paramagnon mass $m$ for a fixed value of the coupling constant $\lambda$. We observe a similarity between the various compounds that we have tested. In a wide range at low value of the mass, the SU(2) degeneracy between $\chi$ and $\Delta$ is verified within a few percents. The existence of such a regime is an indication that a PG driven by SU(2) symmetry is possible in cuprate superconductors. As the mass is increased we progressively lose the level degeneracy with the parameter $\chi$ abruptly dropping down while the paring $\Delta$ is asymptotically going down to zero when the mass increases. It is interesting to see that the SU(2) symmetry is weak for the electron doped and Hg1201 compound which experimentally show much weaker signs of charge order[22,39]. We also find that the compound Bi2212 behaves sightly different than the other compounds in Fig. 3 and 4, although it is not clear at the current stage where this deviation comes from. In Fig. 3b) the level splitting is directly shown for all the compounds and the two regimes, the one at low mass where the SU(2) symmetry is obtained and the higher mass regime where $|\chi-\Delta|/\Delta$ becomes of order one are clearly seen. Within the non linear $\sigma$-model associated to the present theory[9], the SU(2) regime is a signature of the PG of the system, while the energy splitting of the two levels is associated to the superconducting $T_c$. We see that Fig. 3a) mimics the generic phase diagram of the cuprates where the PG line $T^*$ abruptly plunges inside the SC dome at some value of oxygen doping.

Although it is very encouraging to see that the SU(2) regime has a non-zero probability to exist, one can wonder whether the paramagnon mass in hole doped cuprate superconductors is small, since typically the AF correlation length is of few lattice constants[40]. The issue is addressed in Fig. 4a), where the values of $\chi$ and $\Delta$ are shown for a fixed mass as a function of the coupling constant $\lambda$. Here again a generic pattern emerges. For small $\lambda$ the SU(2) symmetry is broken, but surprisingly, above a certain threshold of $\lambda$, the SU(2) symmetry is almost completely restored. As seen in Fig. 4a), the bigger the mass is, the stronger the coupling constant needs to be for the symmetry to be restored. Figure 4b) shows that this behavior is quite general among the different compounds. Note however that the electron -doped compound is less sensitive to the effect of increasing the coupling constant, compared to the other hole-doped ones, for which the SU(2) symmetry is restored for large enough $\lambda$.

### B. Spacial dependence of the splitting

The SU(2) symmetry is not only broken due to the curvature of the Fermi surface at the hot spots, but it is typically broken in the BZ away from the eight hot spots. Figure 5 shows the typical shape of $|\chi|$ and $|\Delta|$ for four compounds under investigation for the most unfavorable case for the symmetry, that is for small values of the mass and coupling constant. The level splitting is shown as a density plot in the bottom. It is rather small almost everywhere in the BZ and at the hotspot positions with maxima of the order of 20-40% around the "shadow" Fermi surface. The main learning from these plots is that the variations of the Fermi surface geometry gives a rather small departing from the SU(2)-degeneracy for a various range of compounds. In all cases, the SU(2) symmetry is well respected at the hotspot positions.

In Fig. 6 we place ourselves in the strong coupling and strong mass regime and plot the variation of $|\chi|$ , $|\Delta|$ and $|\chi-\Delta|/\Delta$. The level splitting is also shown in Fig. 6 and found to be much smaller than the previous case in Fig. 5, and has dropped to an order of 5-10%[41]. Interestingly, the typical shape of $|\chi|$ and $|\Delta|$ in the BZ has changed compared to Fig. 6, with maxima now around the zone edge. This is the justification that "hot regions" instead of "hot spots" is the correct description of hole doped cuprate superconductors within the spin-fermion model. Note that since the maximum of $|\chi|$ is now at the zone edge, the wave vector corresponding to the associated charge order is now parallel to the $x/y$ axes of the system, in similarity with the findings of Ref. [12].

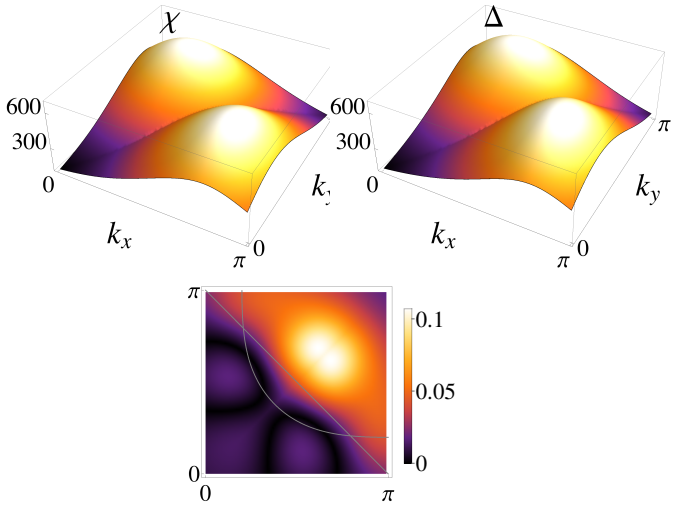


FIG. 6. (Color online) Generic picture of the gap functions $|\chi|$, $|\Delta|$ and $|\chi-\Delta|/|\Delta_{\max}|$ in the first BZ for hole-doped cuprates, here explicitly shown for YBCO. The figures correspond to the large mass and large coupling limit ($\lambda = 160$ and mass $m = 0.5$, so that $E_0 \simeq 160\,\mathrm{K}$ and $E_{\mathrm{eff}} = 226\,\mathrm{K}$) where the SU(2) symmetry is well respected.

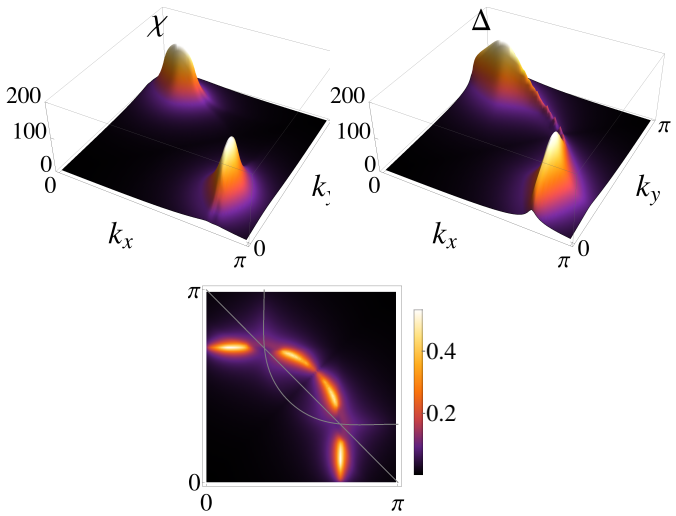


FIG. 7. (Color online) Generic picture of the gap functions $|\chi|$, $|\Delta|$ and $|\chi-\Delta|/|\Delta_{\max}|$ in the first BZ for electron doped materials. The figures correspond to the small mass and small coupling limit ($\lambda = 40$ and mass $m = 10^{-3}$, so that $E_0 \simeq 40\,\mathrm{K}$ and $E_{\mathrm{eff}} = 1265\,\mathrm{K}$) that is most unfavorable for the SU(2) symmetry.

### C. Global trends in cuprate superconductors

The interplay between mass and coupling allows us to relate global trends in the phase diagram for cuprate superconductors with the strength of the SU(2) symmetry breaking. In the electron doped compounds the coupling between AF modes and conduction electrons is believed to be weaker than for the hole doped case. From the above analysis we find that the SU(2) symmetry is less respected in that case leading to a smaller PG dome and overall smaller SC, see Fig. 7. For the same reasons La compounds where the coupling is also believed to be small behave similarly. On the other hand, hole-doped cuprates like YBCO live in the large mass and large coupling regime. This results in broad gapped regions in the BZ where the symmetry is well respected so that both the PG and SC dome are large, as shown in Fig. 6.

Finally, let us mention that a major effect of a magnetic field is to invert the order of the level splitting between the CDW and the SC components[10,11]. This will favor the charge order compared to the SC pairing. We believe that Umklapp scattering can have a similar effect to invert the level ordering, but leave detailed investigation for further studies.

## IV. CONCLUSION

In conclusion, this paper gives firm ground to the intuition that the charge sector is a key player in the physics of cuprate superconductors. While the main instability is still the AF ordering, the $d$-wave bond order relates to the $d$-wave pairing through an SU(2) symmetry. We have shown that there exists a wide range of parameters where the SU(2) degeneracy is fulfilled, which gives a natural explanation for the large PG regime observed in certain compounds. We argue that compounds like electron doped cuprates or the La compounds are outside the regime of SU(2) degeneracy, and the

more pronounced energy splitting is the reason for the weaker PG regime.

## V. ACKNOWLEDGMENTS

We acknowledge discussions with A. Chubukov, S. Kivelson, H. Alloul, P. Bourges, Y. Sidis, A. Sacuto, and V. S. de Carvalho. We thank the KITP, Santa Barbara and the IIP, Natal for hospitality during the elaboration of this work. This work was supported by LabEx PALM (ANR-10-LABX-0039-PALM), of the ANR project UNESCOS ANR-14-CE05-0007, as well as the grant Ph743-12 of the COFECUB which enabled frequent visits to the IIP, Natal. Numerical calculations were carried out with the aid of the Computer System of High Performance of the IIP and UFRN, Natal, Brazil.

[1] P. A. Lee, N. Nagaosa, and X.-G. Wen, Rev. Mod. Phys. **78**, 17 (2006).
[2] E. Gull, O. Parcollet, and A. J. Millis, Phys. Rev. Lett. **110**, 216405 (2013).
[3] S. Sorella, G. B. Martins, F. Becca, C. Gazza, L. Capriotti, A. Parola, and E. Dagotto, Phys. Rev. Lett. **88**, 117002 (2002).
[4] M. R. Norman and C. Pépin, Rep. Prog. Phys. **66**, 1547 (2003).
[5] A. Abanov, A. V. Chubukov, and J. Schmalian, Adv. Phys. **52**, 119 (2003).
[6] A. Chubukov, D. Pines, and J. Schmalian, in *Superconductivity*, edited by K. Bennemann and J. Ketterson (Springer Berlin Heidelberg, 2008).
[7] Close to a magnetic instability, the Spin-Fermion model should capture the relevant low-energy physics of the Hubbard model with arbitrary interaction strength, see e.g. Ref. [6].
[8] M. A. Metlitski and S. Sachdev, Phys. Rev. B **82**, 075128 (2010).
[9] K. B. Efetov, H. Meier, and C. Pépin, Nat. Phys. **9**, 442 (2013).
[10] H. Meier, M. Einenkel, C. Pépin, and K. B. Efetov, Phys. Rev. B **88**, 020506 (2013).
[11] M. Einenkel, H. Meier, C. Pépin, and K. B. Efetov, Phys. Rev. B **90**, 054511 (2014).
[12] H. Meier, C. Pépin, M. Einenkel, and K. B. Efetov, Phys. Rev. B **89**, 195115 (2014).
[13] J. E. Hoffman, E. W. Hudson, K. M. Lang, V. Madhavan, H. Eisaki, S. Uchida, and J. C. Davis, Science **295**, 466 (2002).
[14] N. Doiron-Leyraud, C. Proust, D. LeBoeuf, J. Levallois, J.-B. Bonnemaison, R. Liang, D. A. Bonn, W. N. Hardy, and L. Taillefer, Nature **447**, 565 (2007).
[15] W. D. Wise, M. C. Boyer, K. Chatterjee, T. Kondo, T. Takeuchi, H. Ikuta, Y. Wang, and E. W. Hudson, Nat. Phys. **4**, 696 (2008).
[16] S. E. Sebastian, N. Harrison, R. Liang, D. A. Bonn, W. N. Hardy, C. H. Mielke, and G. G. Lonzarich, Phys. Rev. Lett. **108**, 196403 (2012).
[17] G. Ghiringhelli, M. Le Tacon, M. Minola, S. Blanco-Canosa, C. Mazzoli, N. B. Brookes, G. M. De Luca, A. Frano, D. G. Hawthorn, F. He, T. Loew, M. M. Sala, D. C. Peets, M. Salluzzo, E. Schierle, R. Sutarto, G. A. Sawatzky, E. Weschke, B. Keimer, and L. Braicovich, Science **337**, 821 (2012).
[18] T. Wu, H. Mayaffre, S. Krämer, M. Horvatić, C. Berthier, P. L. Kuhns, A. P. Reyes, R. Liang, W. N. Hardy, D. A. Bonn, and M.-H. Julien, Nat. Commun. **4**, 2113 (2013).
[19] D. LeBoeuf, S. Kramer, W. N. Hardy, R. Liang, D. A. Bonn, and C. Proust, Nat. Phys. **9**, 79 (2013).
[20] M. Le Tacon, A. Bosak, S. M. Souliou, G. Dellea, T. Loew, R. Heid, K.-P. Bohnen, G. Ghiringhelli, M. Krisch, and B. Keimer, Nat. Phys. **10**, 52 (2014).
[21] L. E. Hayward, D. G. Hawthorn, R. G. Melko, and S. Sachdev, Science **343**, 1336 (2014).
[22] W. Tabis, Y. Li, M. Le Tacon, L. Braicovich, A. Kreyssig, M. Minola, G. Dellea, E. Weschke, M. J. Veit, M. Ramazanoglu, A. I. Goldman, T. Schmitt, G. Ghiringhelli, N. Barišić, M. K. Chan, C. J. Dorow, G. Yu, X. Zhao, B. Keimer, and M. Greven, Nat. Commun. **5**, 5875 (2014).
[23] R.-H. He, M. Hashimoto, H. Karapetyan, J. D. Koralek, J. P. Hinton, J. P. Testaud, V. Nathan, Y. Yoshida, H. Yao, K. Tanaka, W. Meevasana, R. G. Moore, D. H. Lu, S.-K. Mo, M. Ishikado, H. Eisaki, Z. Hussain, T. P. Devereaux, S. A. Kivelson, J. Orenstein, A. Kapitulnik, and Z.-X. Shen, Science **331**, 1579 (2011).
[24] I. M. Vishik, M. Hashimoto, R.-H. He, W.-S. Lee, F. Schmitt, D. Lu, R. G. Moore, C. Zhang, W. Meevasana, T. Sasagawa, S. Uchida, K. Fujita, S. Ishida, M. Ishikado, Y. Yoshida, H. Eisaki, Z. Hussain, T. P. Devereaux, and Z.-X. Shen, PNAS **109**, 18332 (2012).
[25] Y. Wang and A. Chubukov, Phys. Rev. B **90**, 035149 (2014).
[26] D. F. Agterberg, D. S. Melchert, and M. K. Kashyap, Phys. Rev. B **91**, 054502 (2015).
[27] P. A. Lee, Phys. Rev. X **4**, 031017 (2014).
[28] E. Fradkin, S. A. Kivelson, and J. M. Tranquada, arXiv:1407.4480 [cond-mat.supr-con] (2014).
[29] X. Montiel, T. Kloss, C. Pépin, S. Benhabib, Y. Gallais, and A. Sacuto, arXiv:1504.03951 [cond-mat.supr-con] (2015).
[30] E. Demler, W. Hanke, and S.-C. Zhang, Rev. Mod. Phys. **76**, 909 (2004).
[31] C. Pépin, V. S. de Carvalho, T. Kloss, and X. Montiel, Phys. Rev. B **90**, 195207 (2014).
[32] Y. Wang, D. F. Agterberg, and A. Chubukov, Phys. Rev. B **91**, 115103 (2015); Y. Wang, D. F. Agterberg, and A. Chubukov, arXiv:1501.07287 [cond-mat.str-el] (2015).
[33] M. R. Norman, Phys. Rev. B **75**, 184514 (2007).
[34] Y. He, Y. Yin, M. Zech, A. Soumyanarayanan, M. M. Yee, T. Williams, M. C. Boyer, K. Chatterjee, W. D. Wise, I. Zeljkovic, T. Kondo, T. Takeuchi, H. Ikuta, P. Mistark, R. S. Markiewicz, A. Bansil, S. Sachdev, E. W. Hudson, and J. E. Hoffman, Science **344**, 608 (2014).
[35] K. Fujita, C. K. Kim, I. Lee, J. Lee, M. Hamidian, I. A. Firmo, S. Mukhopadhyay, H. Eisaki, S. Uchida, M. J. Lawler, E. A. Kim, and J. C. Davis, Science **344**, 612 (2014).
[36] T. Das, Phys. Rev. B **86**, 054518 (2012).
[37] D. Sénéchal and A.-M. S. Tremblay, Phys. Rev. Lett. **92**, 126401 (2004).
[38] We have checked that this approximation is reliable to calculate the spacial distribution of the gap functions.
[39] R. Comin, R. Sutarto, F. He, E. da Silva Neto, L. Chauviere, A. Frano, R. Liang, W. N. Hardy, D. Bonn, Y. Yoshida, H. Eisaki, J. E. Hoffman, B. Keimer, G. A. Sawatzky, and A. Damascelli, arXiv:1402.5415 [cond-mat.supr-con] (2014).
[40] V. Hinkov, S. Pailhes, P. Bourges, Y. Sidis, A. Ivanov, A. Kulakov, C. T. Lin, D. P. Chen, C. Bernhard, and B. Keimer, Nature **430**, 650 (2004).
[41] The gap functions and level splitting of the other compounds are very similar and therefore not shown in Fig. 6.